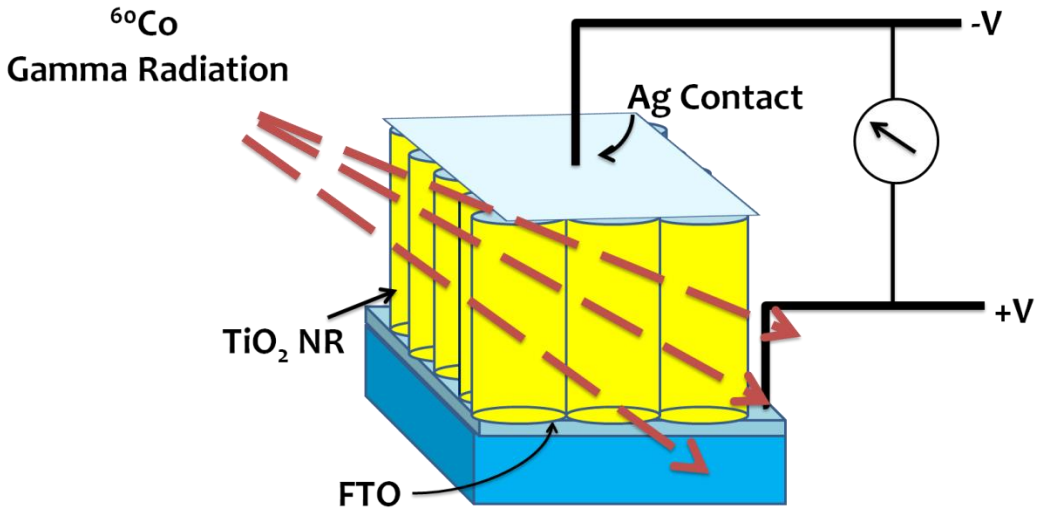

Gamma Radiation Measurement using Hydrothermally Grown TiO_2 Nanorods

Chapter 8 Gamma Radiation Measurement using Hydrothermally Grown TiO2 Nanorods

8.1 Introduction

TiO_2 is also a wide bandgap semiconductor, found in three crystal structures anatase, rutile and brookite. It has huge potential in optoelectronic and chemical applications, such as photovoltaic cells (Bai et al., 2014), production of hydrogen using photocatalytic splitting of water (Chiarello et al., 2017), sensor applications (Bai and Zhou, 2014), cancer treatment (Selin and Cigir, 2019), antimicrobial (Jadiyappa, 2012) and UV Protection (Trivedi and Murase, 2017). TiO_2 nanostructures can be synthesized using various methods such as Sol-gel, CVD, electrochemical, hydrothermal (Khataee and Mansoori, 2012b), thus providing flexibility in manipulating their geometrical shape and sizes different applications.

In this chapter, we report the preparation of TiO_2 Nanorods over FTO substrate using a low-cost and easily scalable hydrothermal method. Structural properties investigated using XRD confirmed the rutile phase of highly oriented (002) TiO_2 nanorods. The rutile phase is also confirmed by Raman spectroscopy, showing the vibrational modes for the rutile phase. Microstructure properties were investigated by scanning electron microscopy showing the uniform deposition of nanorods over the substrate with a diameter ~20-80 nm. Bandgap measured using diffused reflectance is obtained as 3.14 eV. Average carrier lifetime was measured by photoconductive method comes out 78 s. Gamma radiation measurements were performed using a ^{60}Co gamma radiation source. I-V characteristics are carried out on 375 mGy to 3000 mGy gamma-irradiated TiO_2 NR samples. It is observed that leakage current is increasing linearly with respect to irradiated dose.

8.2 Experimental Procedure

The FTO coated glass substrate is cleaned by ultrasonication with methanol followed by rinsing with DI water. Solution of TTIP (Ti^{4+} precursor, 0.005M) precursor in iso propanol. Few drops of the solution were then poured on the substrate and spin-coated. After deposition of a uniform layer of the solution, the substrate is heated up to 500^0C for two hrs in open ambient conditions. This leads to the formation of the TiO_2 seed layer over FTO/Glass. To grow TiO_2 nanorods over this seed substrate, a solution of HCl and DI water in a 1:1 volume ratio is prepared in a Teflon-lined autoclave. Titanium isopropoxide is then added dropwise in solution in suitable concentrations. The solution is continuously stirred for a duration of 30 minutes to get homogeneous mixing of the precursor. The seed substrate is then kept at an angle 45^0 against the wall of Teflon lined autoclave. The autoclave then closed properly and kept at 160 ^{0}C for 8 hrs in an oven. The autoclave is then taken outside from the oven and allowed to cool down to room temperature. The substrate was removed from the autoclave, cleaned with DI water and dried to obtain TiO_2 Nanorods. The prepared nanorods were characterized by X-ray diffraction (XRD) for structural properties, scanning electron microscopy (SEM) for micro structural properties, Raman and UV-Vis spectroscopic measurements to understand the optical properties of TiO_2 Nanorods. Average photo-induced carrier lifetime is investigated by photoconductive measurement. Silver contacts are made at top of the TiO2 nanorods using silver paste for the gamma radiation dosimetry study. The current-voltage (I-V) measurements are carried out using different voltages ranging from +1V to -1V in 201 steps. The gamma exposure on these nanorods is explained schematically in figure 8.1 (a) and all the exposure

experiments are performed in NABL accredited testing and calibration facility using ^{60}Co gamma radiation source (activity ~20 Ci). The test bench consists of source and sample mounting stage on a movable platform to the varying source to sample distances. All exposures are carried out at 150 mGy/hr dose rate for 15, 30, 60 and 120 min durations and I-V characteristics are measured after each exposure simultaneously, as shown schematically in figure 8.1(b). The electrical contacts are extended to the Keithley SMU 2636 and the electrical response was recorded automatically by varying voltage across the sample.

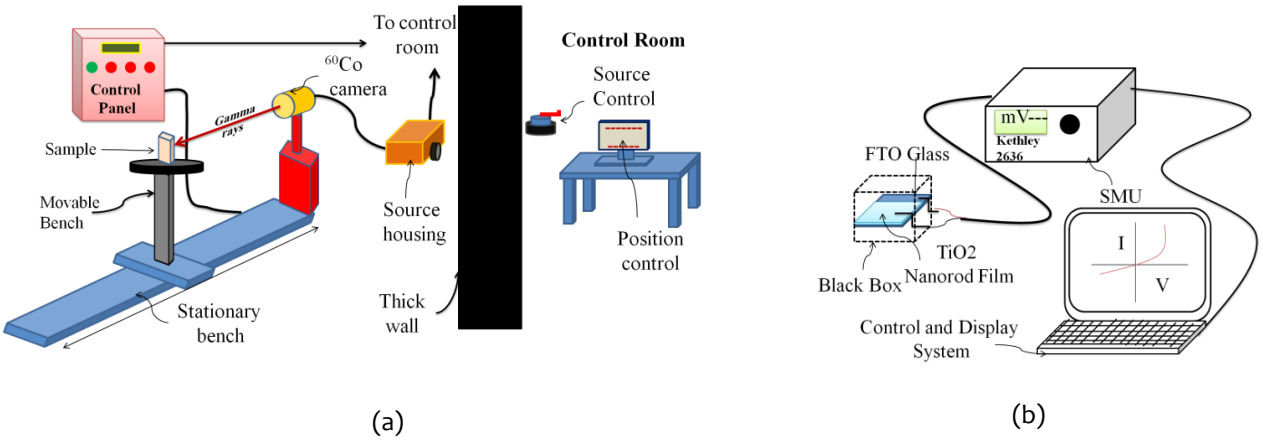

Figure 8.1: (a) Schematic diagram of sample exposure at NABL Accredited Gamma Testing and Calibration Facility (at Defence Laboratory Jodhpur, India) (b) Experimental set-up for I-V measurements on gamma ray exposed TiO_2 nanorod samples

8.3 Results and Discussion

8.3.1 X-ray diffraction (XRD) measurement:

Bruker D8 Advance X-ray diffractometer employing with monochromatic Cu Kα (1.54 Å) incident X-rays as the source in 20°- 80° range at slow scan rate has been used for XRD measurements. The recorded XRD pattern is shown in figure 8.2. We observed a pure rutile phase with diffraction at 36.05°, 62.89° and 69.87° angles, correspond to (110), (002) and (112) planes, respectively, which is in agreement with ICDD file #21-1276. Further, there are additional diffraction peaks at around 26.42°, 33.57°, 37.72°, 54.33°, 57.77° and 65.8°, which correspond to FTO/glass substrate and marked with * in the diffraction pattern to distinguish from TiO_2 diffraction planes. Interestingly, the (002) diffraction peak intensity is very high, suggesting that the TiO_2 nanorods are highly textured along the (002) diffraction plane.

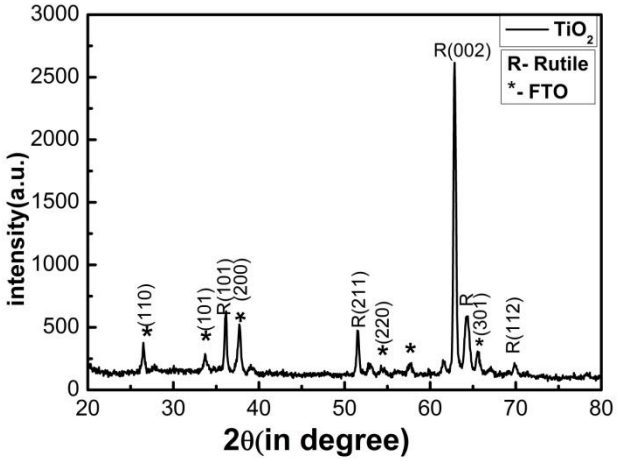

Figure 8.2: X-ray diffraction (XRD) pattern of TiO_2 nanorods grown on FTO/glass substrate, showing highly textured (002) TiO_2nanorods

8.3.2 Scanning Electron Microscopy measurement:

Micrograph recorded from field emission scanning electron microscope (FESEM) for investigating the microstructural evolution and surface features on TiO_2/FTO/glass samples is shown in figure 8.3. Figure 8.3(a), collected at low magnification, 5 kX, is showing nanorods are uniformly distributed on FTO/glass substrates with very high surface density. Further, a higher magnification image, figure 8.3(b), collected at 50 kX shows the partially oriented nanorods, consistent with the XRD observations, showing (002) plane texturing. These nanorods' diameter ranges from 20 nm to 80 nm, as marked in figure 3(b).

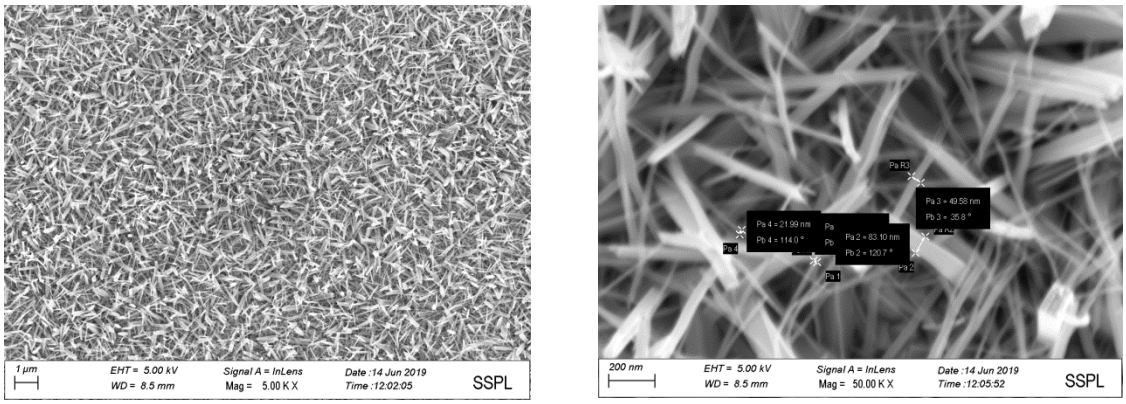

(a) (b)

Figure 8.3: SEM micrographs of TiO_2nanorods grown on FTO/glass substrate at different magnification (a) at 5 kX and (b) 50 kX

8.3.3 Raman and UV-Vis Spectroscopic measurements:

Raman spectroscopic measurements are performed using a green monochromatic (514.5 nm wavelength) light source on synthesized rutile phase TiO_2 nanorods on FTO/glass substrate. The collected Raman spectrum of TiO_2 nanorods/FTO/glass along with bare FTO/glass substrate is shown in figure 8.4(a). The rutile phase of TiO_2 corresponds to P42/mnm tetragonal space group, consisting of two formula units, i.e., two titanium atoms at (0, 0, 0) and (½, ½, ½), whereas four oxygen atoms at (u, u, 0), (-u, –u, 0), (½+u, ½-u, ½) and (-½-u, -½+u, -½), respectively. As per the factor group analysis at Γ point in the reciprocal lattice, four Raman active modes as $\Gamma_{opt} = A_{1g} + B_{1g} + B_{2g} + E_g$ and four infrared active modes as $A_{2u} + 3E_u$ are found. The vibrational frequencies of these Raman active modes are observed at 612 cm^{-1} (A_{1g}), 236 cm^{-1} (B_{1g}),827 cm^{-1} (B_{2g}) and 448 cm^{-1} (E_g). We observed three vibrational Raman modes at 237.49 cm^{-1}, 444.02 cm^{-1}, 608.59 cm^{-1} correspond to B_{1g}, E_g and A_{1g} Raman vibration modes, respectively for the synthesized TiO_2 nanorods, substantiating the observed rutile crystallographic phase from XRD(Mokhtar and Nafarizal, 2016). Further, a mode observed at 325.09 cm^{-1} peak is attributed to fluorine-doped tin oxide's vibrational mode and is usually observed as background for thin films on FTO/glass substrates.

Further, we used Carry 4000 UV-Vis spectrophotometer to collect the diffuse reflectance in the UV-Vis range (0.2 to 0.9 µm). The reflectance is converted into absorbance (α) using the Kubelka-Munk model and Tauc plot, i.e., $(\alpha.E)^2$ versus energy E (=hν) is plotted in figure 8.4(b). The straight line region is extrapolated to $(\alpha.E)^2 = 0$, as shown by the red line to estimate the bandgap and is 3.14 eV for synthesized TiO_2 nanorods.

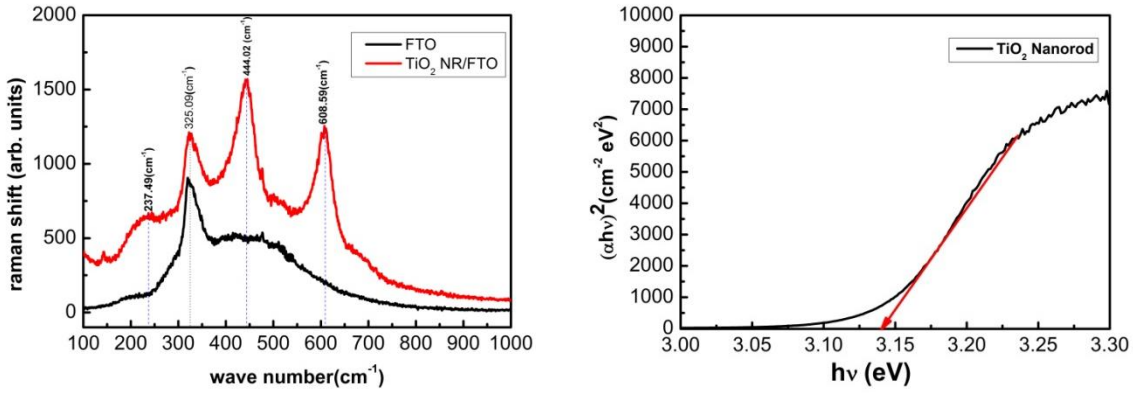

(a) (b)

Figure 8.4: Room temperature (a) Raman Spectra and (b) computed (α.E)² versus energy E (= hν) plot for synthesized rutile TiO_2nanorods

8.3.4 Photo Induced Carrier Lifetime measurement

Photo induced carrier lifetime of TiO_2 nanorods investigated using the photoconductive decay method. TiO_2 nanorods is exposed to fluorescent light of intensity $1.87x10^4$ Lux at -1V biasing and current is measured continuously at a time step of 1 second. Electrons raised to the conduction band due to exposure of light, leading to drastic increase in current, which saturates as time progresses. After one hour, when the light exposure is off, an exponential decay in current is observed, which is due to the loss of electrons in the conduction band. The current reaches to background level in ~500 s (figure 8.5). The decay of current to 1/e time occurs in 77.4 s, which is the average lifetime of charge carriers (Inset).

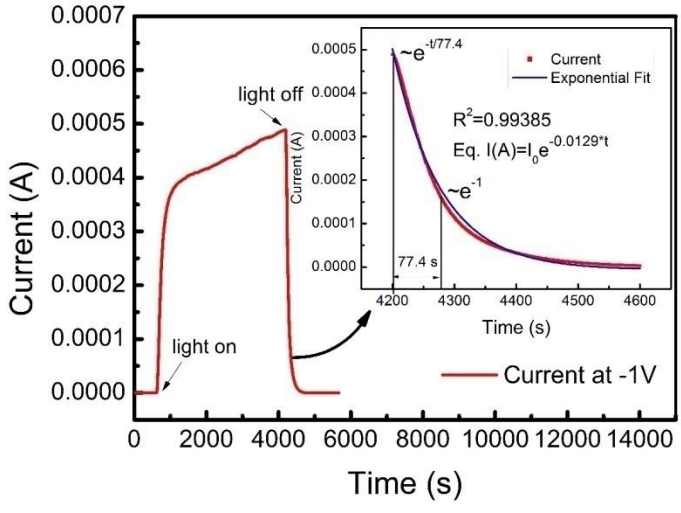

Figure 8.5: Carrier lifetime measurement using photoconductive decay (PCD) method.

8.3.5 Gamma Radiation Dose-Response measurement:

The current-voltage (I-V) characteristics measurement is performed on the Ag/TiO_2NR/FTO samples). The unexposed TiO_2 NR/FTO/glass sample exhibits Schottky characteristics as the work function of the metal contact $Ø_{Ag}$ is greater than that of TiO_2, i.e., $Ø_{TiO2}$. I-V characteristics measured at different gamma doses varying from 370-3000 mGy are shown in figure 5 a. Further, 370 mGy gamma radiation exposure increases the leakage current, which can be seen in contrast with the unexposed sample, figure 8.6 (a). The increase in gamma radiation exposure, i.e., 750 mGy, 1500 mGy and 3000 mGy, showed enhanced leakage current with increasing exposure. The value of current measured for various gamma radiation doses at -1V is shown in figure 8.6 (b), showing a continuous increase in current with increasing absorbed gamma radiation doses.

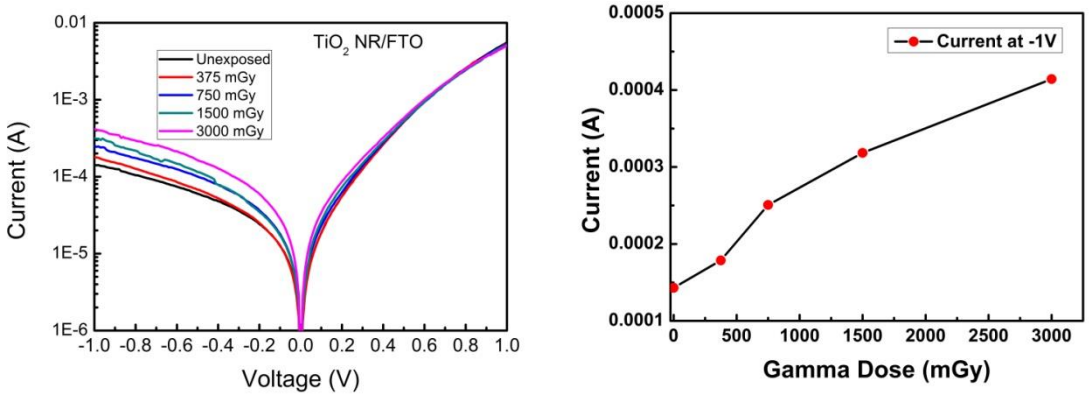

(a) (b)

Figure 8.6: (a) I-V characteristics and (b) current measured at -1V for TiO_2/FTO/glass with silver as top contact at different gamma dose exposures

8.3.6 Mechanism of Gamma Dosimetry using TiO_2nanorods:

Gamma Radiation absorption in TiO_2 nanorods leads to the creation of electron hole pairs due to the photoelectric and Compton scattering process. These primary energetic electrons, traveling in the medium, i.e., TiO_2 nanorods, as explained in figure 8.7 (a), ionize the material further, thus creating secondary electron-hole pairs. The generated electrons do not combine immediately after combine with holes but remain in conduction band due to large carrier lifetime. Further, as TiO_2 nanorods are subjected to reverse bias voltage, as explained schematically in figure 6 (a), electrons are injected from silver metal to TiO_2 nanorods, which recombine with the gamma radiation generated holes and thus, contributing to the extra current with respect to the unexposed TiO_2 nanorod sample. This recombination mechanism is explained schematically using the energy band diagram and electron-hole dynamics in figure 8.7 (b). This recombination increases with increasing gamma dose, showing enhanced leakage current, nearly linear with gamma exposure, as shown in figure 8.6 (b).

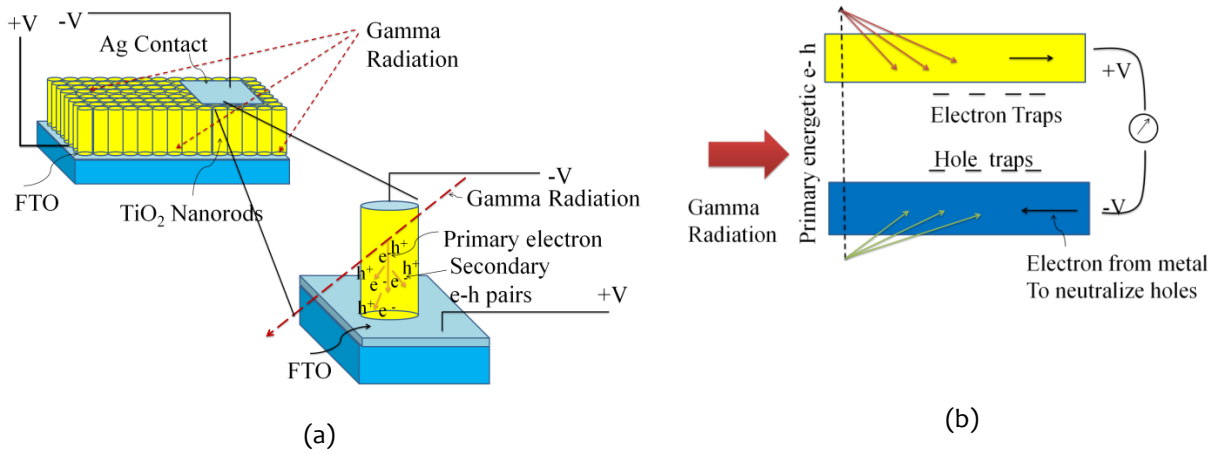

Figure 8.7: (a) The schematic process of gamma radiation exposure to the TiO_2nanorods and creation of e-h pairs together with creation of secondary electrons and (b) electronic band diagram explaining recombination dynamics of gamma radiation generated e-h pairs in TiO_2nanorods

8.4 Conclusion

TiO_2 Nanorods are prepared on FTO/glass substrate using the hydrothermal method. The developed nanorods are of Rutile phase confirmed from XRD, Raman and UV-Vis spectroscopic studies. The developed nanorods are uniformly deposited on the FTO/Glass, ranging from 20-80 nm. Photoconductive measurements show that these Nanorods have a large average photoinduced carrier lifetime. Gamma radiation-induced effects on the developed nanorods investigated using I-V measurement. The measured I-V characteristics showed a nearly linear increase in leakage current with increasing gamma radiation exposure. This linear increase makes TiO_2 nanorods a suitable candidate for low-cost gamma radiation dosimetry applications. Thus, these studies may provide an easily scalable route to fabricate low-cost and efficient TiO_2 nanorod based gamma radiation dosimeters.